

Quantitative spectroscopy of x-ray lines and continua in Tokamaks

N. J. Peacock, R. Barnsley, K. D. Lawson, I. M. Melnick, M. G. O'Mullane et al.

Citation: *Rev. Sci. Instrum.* **68**, 1734 (1997); doi: 10.1063/1.1147983

View online: <http://dx.doi.org/10.1063/1.1147983>

View Table of Contents: <http://rsi.aip.org/resource/1/RSINAK/v68/i4>

Published by the [American Institute of Physics](#).

Related Articles

Diagnostics of underwater electrical wire explosion through a time- and space-resolved hard x-ray source
Rev. Sci. Instrum. **83**, 103505 (2012)

A novel technique for single-shot energy-resolved 2D x-ray imaging of plasmas relevant for the inertial confinement fusion
Rev. Sci. Instrum. **83**, 103504 (2012)

Near-coincident K-line and K-edge energies as ionization diagnostics for some high atomic number plasmas
Phys. Plasmas **19**, 102705 (2012)

X-ray backlight measurement of preformed plasma by kJ-class petawatt LFEX laser
J. Appl. Phys. **112**, 063301 (2012)

Time-resolved soft x-ray spectra from laser-produced Cu plasma
Rev. Sci. Instrum. **83**, 10E138 (2012)

Additional information on *Rev. Sci. Instrum.*

Journal Homepage: <http://rsi.aip.org>

Journal Information: http://rsi.aip.org/about/about_the_journal

Top downloads: http://rsi.aip.org/features/most_downloaded

Information for Authors: <http://rsi.aip.org/authors>

ADVERTISEMENT

ORTEC MAESTRO® V7 MCA Software

For over two decades, MAESTRO has set the standard for Windows-based MCA Emulation. MAESTRO Version 7.0 advances further:

- New!** Windows 7 64-Bit Compatibility with Connections Version 8
- New!** List Mode Data Acquisition for Time Correlated Spectrum Events
- New!** Improved Peak fit calculations
- New!** Improved graphics handling for multiple displays
- New!** Open spectrum files directly from Windows Explorer
- New!** Improved performance with Job Functions and display updates

MAESTRO continues to be the world's most popular nuclear MCA software in a broad range of applications!



**Now 64-bit
Windows 7
Compatible!**

www.ortec-online.com

Quantitative spectroscopy of x-ray lines and continua in Tokamaks^{a)}

N. J. Peacock, R. Barnsley,^{b)} K. D. Lawson, I. M. Melnick,^{c)} M. G. O'Mullane,^{d)}
M. A. Singleton,^{d)} and A. Patel

UKAEA-Fusion (Euratom/UKAEA Fusion Association), Culham Laboratory, Abingdon, Oxfordshire OX14
3DB, United Kingdom

(Received 16 May 1996; accepted for publication 25 November 1996)

Crystal and synthetic multilayer diffractors, deployed either as flat Bragg reflectors, or curved, as in the Johann configuration, are used to study the spectrum of COMPASS-D and other tokamaks in the wavelength region of 1–100 Å. In this article, we concentrate on the measurement of absolute photon fluxes and the derivation of volume emissivities of the lines and continua in the x-ray region. The sensitivities of these instruments to absolute photon flux have been constructed *ab initio* from the individual component efficiencies, including published values of the diffractor reflectivities, which have been checked or supplemented by measurements using a double-axis goniometer or from line branching ratios. For those tokamak plasmas, where the elemental abundances and effective ion charge are documented, the x-ray continuum intensity itself has been used as a calibration source to derive absolute instrument sensitivity, in reasonable agreement with the *ab initio* method. In the COMPASS-D Tokamak, changes in the effective ion charge state, Z_{eff} , have been derived for different operating conditions, from the absolute intensity of the continuum at ~ 4 Å. From the radiances of the line emission, changes in the absolute level of impurities following ‘‘boronization’’ of the vacuum vessel have also been documented. © 1997 American Institute of Physics. [S0034-6748(97)02803-7]

I. INTRODUCTION

In large Tokamaks, such as the Joint European Totus (JET), the radiated power level from the core plasma and the associated effective ion charge, Z_{eff} , are routinely monitored using tomographic reconstruction of bolometer signals and of the visible bremsstrahlung continuum. In much smaller tokamaks, with degraded ion confinement, light from recycling ions near the plasma edge tends to obscure the core emission and these diagnostic techniques become somewhat less secure. Discrimination between the core and the edge radiation is always possible at higher photon energies in the extreme ultraviolet (XUV) and x-ray regions of the spectrum. Indeed, short wavelength spectroscopy is the only method for monitoring the different radiating ion species in the core. This is of some importance when assessing, on the one hand, the effect of impurities on the effective ion charge Z_{eff} on the fuel dilution and on spatial radiation loss patterns, while on the other hand, the effect of gettering, divertor screening, etc. on the impurity influxes. In addition, the impurity line intensities and spectral profiles are a rich source of information on ion transport and on the core plasma environment.^{1–5} In this article, we develop the theme of using the x-ray line and continuum intensities to derive Z_{eff} and the impurity ion abundances, or equivalently, the elemental components of the total radiated power. For this to be feasible, the radiation has to be measured on an absolute basis. The problem then reduces to that of establishing absolute efficiencies of the spectrometers. In the JET and COMPASS-D programs, the x-ray spectrum discussed in this

article is routinely measured using a broadband, Bragg rotor survey (1 Å \leftarrow 100 Å) spectrometer,^{6,7} complemented by a Johann configuration, curved crystal spectrometer,^{8,9} which we term ‘‘(CCD)²’’ and which is ideally suited to line profile analyses.

II. *Ab initio* CALCULATION OF BRAGG ROTOR SPECTROMETER EFFICIENCY

The Bragg rotor spectrometer accommodates a number, up to six, of flat diffractors such as crystals, synthetic multilayers, Langmuir–Blodgett films, distributed around the faces of a hexagon which, in the survey mode, rotates allowing each diffractor to view the plasma emission sequentially. Sharing the viewing aperture is a subsidiary ‘‘paddle’’ or spindle along which up to four diffractors can simultaneously view the plasma. The paddle typically acts in a reciprocating angular scan mode simultaneously with but independently of the rotor. The *ab initio* calibration method^{10,11} involves the construction of the overall instrument efficiency from a consideration of the component efficiencies of the spectrometer such as transmission factors, étendue, integrated crystal reflectivity, and detector efficiency, all as a function of Bragg angle.

A plasma source with a radiance $I(\nu)$ [$\text{W m}^{-2} \text{sr}^{-1} \text{Hz}^{-1}$] will, in the rotating mode with angular frequency ω , give rise to a detector count ‘‘ N ’’ given by

$$N \cdot h\nu = I(\nu) \cdot \frac{R_c}{\omega} \psi_x \psi_y \cdot h_x h_y \cdot \eta_s \eta_\lambda, \quad (1)$$

where the component factors and the instrument layout are discussed by Singleton.¹¹ R_c is the integrated reflectivity of the diffractor, ψ_x and ψ_y are the collimator acceptance angles in and perpendicular to, respectively, the plane of the dispersion; h_x and h_y are the projected height and width, respec-

^{a)}The abstract for this article appears in Rev. Sci. Instrum. **68**, 1063 (1997).

^{b)}Present address: Department of Physics, University of Leicester, UK.

^{c)}Present Address: Department of Physics, University College, London, UK.

^{d)}Present address: Department of Physics, University College, Cork, Ireland.

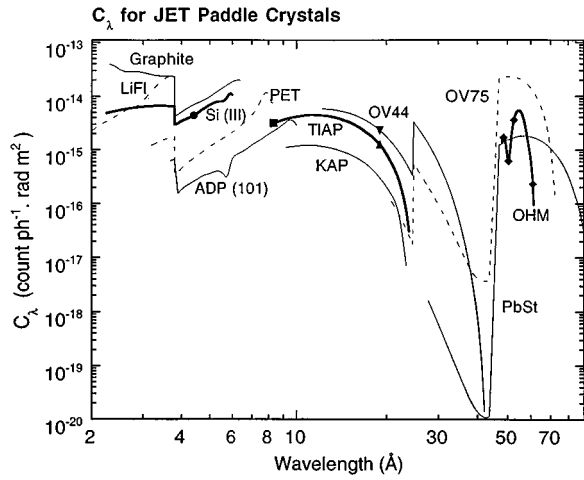


FIG. 1. *Ab initio* calculations of the absolute sensitivity, C_λ against wavelength, of the Bragg rotor paddle spectrometer as used on JET. Published values, where available, of integrated reflectivities for the range of diffractors covering the wavelength range of 1–100 Å, are used in the synthesis of C_λ . The experimental points are values derived in the text.

tively, of the diffractor at the collimator; η_x and η_λ are the transmission of the structural elements and finally the overall detector efficiency. Integrating counts over the line width, the spectrometer sensitivity is defined as

$$S_\nu = \frac{N\omega}{I} \text{ in units of } (\text{counts rad s}^{-1}/\text{Wm}^{-2} \text{ sr}^{-1}). \quad (2)$$

In this article, we define the spectrometer sensitivity as a function of wavelength in terms of an effective étendue, C_λ , where

$$C_\lambda = S_\nu \frac{h\nu}{4\pi} = R_c \frac{\psi_x \psi_y}{4\pi} \cdot h_x h_y \cdot \eta_s \eta_\lambda \quad (3)$$

in units of (counts photon⁻¹ rad m²). In the case where the source is defined in terms of an irradiance $\varepsilon(\lambda) \cdot \Delta Z$ photons s⁻¹ m⁻², where Z is a plasma dimension, then the spectrometer sensitivity is given simply by C_λ :

$$\varepsilon(\lambda) \cdot \Delta z = \frac{N\omega}{C_\lambda}. \quad (4)$$

Of all the components contributing to the over-all spectrometer efficiency, R_c is the most uncertain. We assume published values for the integrated reflectivity and check on these, where possible, using our own data as discussed in Secs. III, IV, and V. Constructions of the overall efficiency of the paddle configuration for the diffractors available during the 1994–95 JET operations⁶ are shown in Fig. 1. R_c values are taken from the work of the Leicester group^{12–16} except for the Si(111) crystal where the data is from the calculations of Henke *et al.*¹⁷ Using the two-crystal diffraction results produced at the University of Leicester, R_c values at discrete wavelengths are fitted to continuous Darwin–Prins functions. Higher order reflection integrals are estimated, where appropriate, also using Darwin–Prins model calculations. The diffractors used in the present Tokamak studies are fresh samples, usually from the same source of supply. The variation in the C_λ values at a given wave-

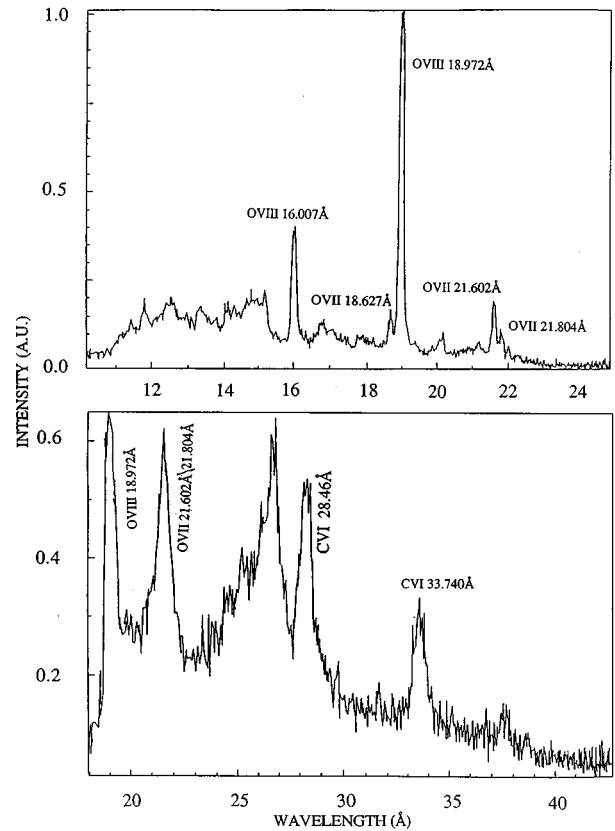


FIG. 2. Overlapping JET spectra of O VIII and O VII recorded simultaneously by the Bragg rotor paddle using multiple diffractor elements such as TIAP (above) and OV44 (below).

length, for example, Si(111) and ADP(101), as illustrated at 4 Å in Fig. 1, reflects not only differences in R_c for these two crystals but more importantly the variation in the geometric factors involved in the different Bragg angles, $\theta_{\text{BRAGG}} = 45^\circ$ for Si(111) and $\theta_{\text{BRAGG}} = 24.7^\circ$ for ADP(101). The overall accuracy of the absolute sensitivities in Fig. 1 is considered to be within approximately $\pm 50\%$, perhaps worse for some of the long wavelength diffractors. In support of our use of the Leicester experimental data, we have checked their R_c values for a few crystals, TIAP¹⁶ at Al K_α , for example, using our new two-axis goniometer,¹⁸ and the agreement is good, generally to within 20%, as indicated by the discrete point at 8.3 Å on the TIAP curve in Fig. 1. Reflectivity data for other diffractors for which there are no published data, such as OV44, an OVONYX (W–Si) multilayer, and the OHM crystal, are inferred from the integrated line intensities of the same transition appearing simultaneously on adjacent

TABLE I. R_c derived from overlapping spectral lines on Bragg rotor spectrometer.

Diffractor	Reference crystal	Wavelength	R_c derived
OV44	TIAP	18.98 Å	1.39×10^{-3} rad
OHM	PbSt	48.59 Å	1.37×10^{-4} rad
		50.43 Å	6.08×10^{-5} rad
		52.69 Å	4.07×10^{-4} rad
OV120	PbSt	75.93 Å	3.70×10^{-3} rad

TABLE II. Comparison of independent calibrations of C_λ for TIAP (100) and Si(111) diffractors per detector channel on the Bragg paddle spectrometer used on JET, in units of counts photon⁻¹ rad m²·10⁻¹⁵.

Diffractor	λ (Å)	Continuum		Absorption		Cross calibration
		irradiance	edge	<i>ab initio</i>		
TIAP(001)	19	1.8	...	1.2	1.7	
Si(111)	4.4	3.3	3.5	3.6	...	

diffractors located on the paddle. An example from JET of the O VII O VIII line spectra overlapping on the OV44 and TIAP diffractors is shown in Fig. 2 and illustrates the technique. A summary of R_c values derived in this way is given in Table I.

III. BRANCHING RATIO AND GONIOMETER DERIVATIONS OF R_c

The OHM crystal exhibits resolving powers comparable with grating spectrometers in the 45 Å (-) 60 Å region and is therefore ideal for monitoring line emission from bottom ions such as B V and B IV. The B IV intercombination line $1s^2-1s2p^3P_1$ at 61.089 Å is readily resolved from the singlet, parent transition at 60.314 Å and has a single branching transition $1s2s^3S_1-1s2p^3P_1$ at 2826.66 Å in the UV which may be used as a transfer standard of radiance.¹¹ The radiance in COMPASS-D of the UV branch of the B IV $1s2p^3P_1$ decay has been calibrated against a radiation-standard D₂ lamp. Both x-ray and UV transitions are observed simultaneously through the Bragg rotor vacuum aperture, the x-ray line being recorded by diffraction from one facet of the rotor, while the UV line is reflected from a mirror placed at the normal position of the diffractor paddle into a grating spectrometer with multichannel read out.¹¹ The integrated efficiency of OHM at 61 Å from this experiment¹¹ is deduced to be 1.6×10^{-3} rad. This value for R_c has been included in the Bragg efficiency plots in Fig. 1. The other points for OHM are from overlapping lines of the tokamak spectrum measured with the PbSt diffractor. The remaining

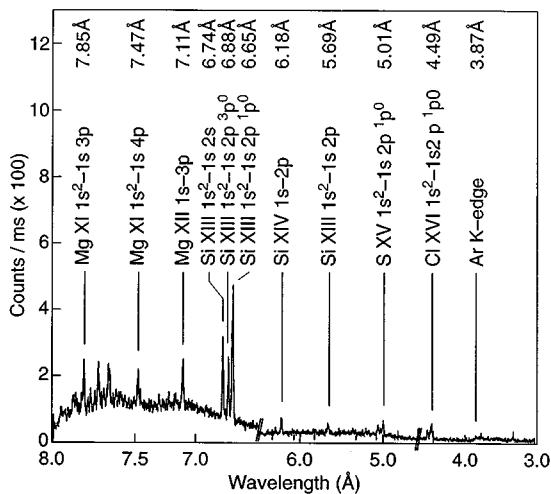


FIG. 3. Tokamak x-ray spectrum using a PET crystal on the Bragg rotor. Note the step in the x-ray continuum due to absorption at the Ar K edge by the gas flow counter.

experimental points in Fig. 1 are deduced using the x-ray continuum from well diagnosed Tokamak discharges as transfer standards, as described below in Secs. IV and VI.

IV. USE OF THE X-RAY CONTINUUM FROM JET AS A TRANSFER STANDARD

Reconstruction of the absolute x-ray continuum signal in terms of Z_{eff} and other plasma parameters has been attempted previously.¹⁹ However, in modern tokamak research, as for example during the 1994–95 JET program, all of the parameters, such as the electron temperature and density profiles, $T_e(r), n_e(r)$, ion transport and impurity abundances, required to calculate the continuum are routinely available. The impurity abundances are derived, at least for a limited range of operating conditions, using a semiempirical technique²⁰ which relies on normalizing the sum of the elemental radiation components (derived from line intensities) to the total radiation bolometer signal. With this information, it is possible to construct the x-ray continuum radiance along an arbitrary line of sight (LOS). The continuum consists of two components, the free-free (bremsstrahlung) and free-bound (recombination) radiation, $I_{\text{CONT}} = I_{\text{ff}} + I_{\text{fb}}$:

$$I_{\text{CONT}} = \frac{h}{4\pi} \left(\frac{c}{\lambda} \right)^2 \frac{\Delta\lambda}{\lambda} \frac{1}{\cos \alpha} \int_{R_1}^{R_2} [\epsilon(\lambda)_{\text{ff}} + \epsilon(\lambda)_{\text{fb}}] \cdot dR, \quad (5)$$

where the LOS integral is taken along a chord with angle α to the major radius, R .

The sum is then related to the signal measured from the Bragg rotor to derive the spectrometer efficiency S_v .

The bremsstrahlung volume emissivity, in units of $\text{W cm}^{-3} \text{Å}^{-1}$, is $\epsilon(\lambda)_{\text{ff}} = 1.9 \times 10^{-28} n_g^2 Z_{\text{eff}} G_{\text{ff}} T_g^{-1/2} \lambda^{-2}$, where G_{ff} is the free-free Gaunt factor. The recombination continua $\epsilon(\lambda)_{\text{fb}}$ are assumed to be H like and are integrated over all n shells with $n \geq Ry \cdot Z^2 / hv$. The ratio of $\epsilon(\lambda)_{\text{fb}} / \epsilon(\lambda)_{\text{ff}}$ is given by

$$\epsilon(\lambda)_{\text{fb}} / \epsilon(\lambda)_{\text{ff}} = \frac{2 \cdot Ry \cdot G_{\text{fb}} \cdot Z_i^2}{T_e \cdot G_{\text{ff}}} \sum_n \left[\frac{1}{n^3} \exp\left(\frac{hc}{T_e \lambda n} \right) \right]. \quad (6)$$

In general, the continuum will be dominated by the bremsstrahlung except perhaps for the spectral regions on the high energy side of $Ry \cdot Z^2$ which cover $\epsilon(\lambda)_{\text{fb}}$ recombination directly into the ground state.

The absolute irradiance of the x-ray continuum has been estimated, as above, using the known plasma parameters on a number of JET discharges and compared with the Bragg paddle signal in order to derive C_λ adjacent to the main resonance lines of Ly α O VIII at 19 Å [TIAP (001)] and Cl XVI at 4.44 Å [Si (III)]. Overlapping orders in the Bragg diffraction have to be taken into account and are particularly significant in the case of the TIAP crystal, where the reflection integrals in orders 1:2:3 scale as 1:0.21:0.087. A comparison of the Bragg paddle efficiencies derived, first from an estimate of the absolute irradiance of the JET continuum and second from an *ab initio* construction, is shown in Table II. Statistical errors in estimates of the continuum irradiance amount to $\pm 30\%$. The biggest uncertainty, however, is the scattered background light level in the paddle spectrometer.

TABLE III. Inventory of impurity abundances derived from line intensities in the Bragg rotor spectrum during pre and postboronization operations in COMPASS-D.

	Preboron- ization	No. 10 postboron- ization	No. 80 postboron- ization	No. 180 postboron- ization
Z_{eff}	2.0	1.2	1.2	1.9
$q_z (z=5) \%$	<0.07	0.14	<0.07	<0.07
$q_z (z=6) \%$	2.27	0.45	0.2	1.9
$q_z (z=8) \%$	0.43	0.07	0.2	0.5

In general, scattered light causes unacceptable errors in the apparent continuum count rate for wavelengths above about 25 Å. A check on the true level of the continuum has been carried out using the drop in the continuum intensity across selected absorption edges, such as the Ar K edge at 3.87 Å illustrated in Fig. 3. The absorption edge technique for assessing the continuum intensity gives, surprisingly, a somewhat increased value of C_λ , but both values are still within the 50% error estimate of the *ab initio* value. Confirmation of the *ab initio* sensitivity for the TIAP crystal at 19 Å is obtained by cross calibration with an absolutely calibrated XUV spectrometer, of the type described by Schwob *et al.*,²¹ viewing the same plasma.

V. DERIVATION OF Z_{eff} FROM LINE INTENSITIES IN COMPASS-D

Having established the absolute efficiency of the Bragg rotor survey spectrometer, the integrated counts over the line profile can be related, by Eq. (3), to the volume emissivity of a selected transition and hence via ionization balance to the ion concentration $q_z = N(z)/n_e$ through the relation

$$\epsilon(\lambda) = n_e^2 q_z C_{ij}, \quad (7)$$

where C_{ij} is the effective excitation rate. The concentration of the main impurities in COMPASS-D has been assessed¹¹ throughout a program of boronization using glow discharges

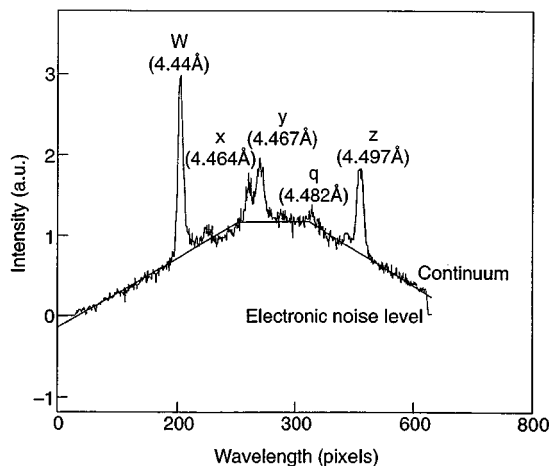


FIG. 4. The x-ray continuum underlying the Cl XVI ($1s^2-1s\ 2p$) line spectrum from COMPASS-D is emphasized by ground-state recombination light from neon ions following gas injection. The trapezoidal intensity function is due to vignetting by the finite port aperture when viewing tangentially.

in $B(\text{CD}_3)_3$ and the results are summarized in Table III. From the q_z values, the $Z_{\text{eff}} = 1 + \sum q_z \cdot Z(Z-1)$, values are readily deduced. It is clear that direct contamination of the plasma, by carbon and boron, is minimal immediately following boronization and that the overall reduction in impurity content lasts for some 200 discharges.

VI. THE X-RAY CONTINUUM FROM COMPASS-D AT 4.44 Å

In experiments aimed at measuring toroidal plasma rotation in COMPASS-D⁹ the (CCD)² spectrometer, using a Si(III) crystal, viewed the plasma tangentially to the major radius through a narrow vacuum aperture. The limited angular acceptance of the entrance optics resulted in vignetting of

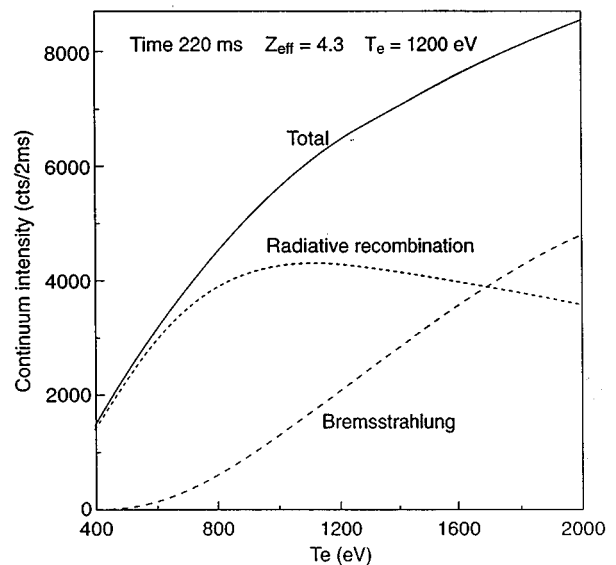
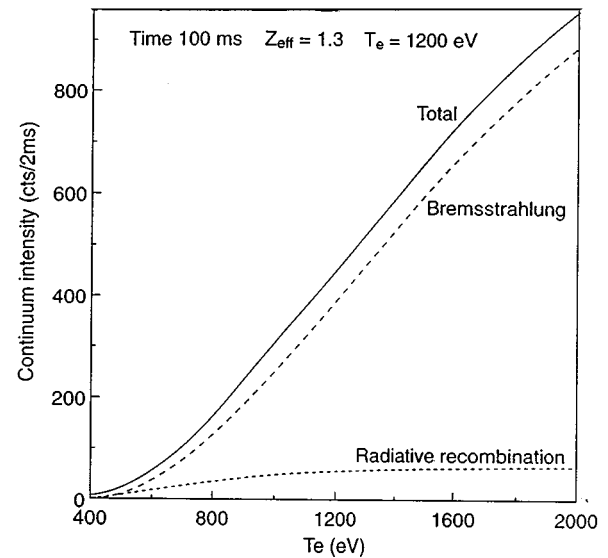


FIG. 5. Calculations of the bremsstrahlung and recombination continuum signals at 4.4 Å on COMPASS-D as recorded by the *ab initio*, absolutely calibrated (CCD)² spectrometer. The relatively high Z_{eff} in the lower figure results from the dominant contribution of free-bound recombination following neon injection. The value of Z_{eff} derived in the upper figure refers to a time period in the same discharge prior to neon injection and is more typical in boronized, high density tokamak discharges.

the spectrum between 4.44 and 4.50 Å. The resulting trapzoidal aperture function is readily seen in Fig. 4 when neon puffing enhanced the underlying background continuum. A band-pass, $\Delta\lambda=5.3$ mÅ units wide, on the short wavelength side of the 4.4436 Å “w” line is chosen as a convenient line-free, spectral region²² over which the continuum intensity could be modeled as outlined in Sec. IV, but with ion abundances and therefore Z_{eff} as adjustable parameters. Calculation of the bremsstrahlung emission is relatively straightforward. However, the free bound recombination has to be summed over all ion charge states in the LOS. In practice, we consider only elements which, from the Bragg rotor survey studies, we know to be abundant and restrict our calculations to the nuclei, H and H-like ions of the elements D, B, C, O (and Ne, where applicable). The locations of these ions in $T_e(r), n_e(r)$ space are calculated using an appropriate ion transport code.⁹ Again, *ab initio* construction of the sensitivity of the (CCD)² spectrometer diagnostic system has been synthesized from its component efficiencies and apertures.⁹ The value of R_C adopted for first order diffraction from Si(111) at 4.4 Å is 1.3×10^{-4} rad in the COMPASS continuum experiments, Melnick (1995).⁹ A somewhat smaller reflection integral, 0.9×10^{-4} rad, has been used in the *ab initio* construction of the paddle C_λ . The concentrations of the ions are then adjusted to fit the observed count rate at 4.44 Å. With no gas puffing, bremsstrahlung dominates the emission, Fig. 5. Following neon gas puffing at a later time during the same discharge, radiative recombination into the ground states of the Ne ions dominates the signal, Fig. 5. A core neon abundance q_z ($z=10$) of 3% and $Z_{\text{eff}}=4.3$ are deduced. For H-mode confinement in high density, $n_e > 5 \times 10^{19} \text{ m}^{-3}$, freshly boronized discharges, the continuum intensity predicts $Z_{\text{eff}} \cong 1.3$, in pleasing agreement with the values derived from the line intensities recorded using the Bragg rotor, Table III.

VII. DISCUSSION

In small or medium-sized tokamaks, where visible emission tomography is not routinely available for deriving the relatively weak core continuum intensity, the x-ray spectrum can be used to distinguish the core emission from light at the plasma boundary. Analysis of the x-ray line and continuum features in terms of the elemental abundances and therefore Z_{eff} is somewhat tortuous but the main uncertainties relate to the absolute efficiency of the spectrometer and to our confidence in the electron profiles and ion transport. This article demonstrates that using x-ray spectrometers, calibrated

against absolute photon fluxes to within $\pm 50\%$, analyses of the line and continuum irradiances yield self-consistent values of the core impurity parameters for a medium-sized tokamak, such as COMPASS-D.

ACKNOWLEDGMENTS

This work is jointly funded by the U.K. Department of Trade and Industry and EURATOM.

- ¹E. Kallne and J. Kallne, *Phys. Scr.* **T17**, 152 (1987).
- ²N. J. Peacock, *Astrophys. Space Sci.* **237**, 341 (1996).
- ³N. J. Peacock *et al.*, in *Proceedings of 21st EPS Conference on Controlled Fusion and Plasma Physics, Montpellier, France*, edited by E. Joffrin, P. Platz, and P. Stott (CEA Cadarache on behalf of European Physical Society, Europhysics Conference Abstracts, 1994), Vol. 18B, part I, p. 134.
- ⁴N. J. Peacock *et al.*, in *Proceedings of 22nd EPS Conference on Controlled Fusion and Plasma Physics, Bournemouth, England*, edited by B. Keen, P. Stott, and J. Winter (JET Undertaking, Abingdon, UK on behalf of European Physical Society, Europhysics Conference Abstracts, 1995), Vol. 19C, part I, p. 97.
- ⁵R. Barnsley *et al.*, *UV and X-ray Spectroscopy of Laboratory and Astrophysical Plasmas*, edited by E. Silver and S. Khan (Cambridge University Press, Cambridge, 1993), p. 513.
- ⁶R. Barnsley *et al.*, in *Proceedings of 22nd EPS Conference on Controlled Fusion and Plasma Physics, Bournemouth, England*, edited by B. Keen, P. Stott, and J. Winter (JET Undertaking, Abingdon, UK on behalf of European Physical Society, Europhysics Conference Abstracts, 1995), Vol. 19C, part I, p. 81.
- ⁷R. Barnsley, Ph.D. thesis, University of Leicester, (1993).
- ⁸A. F. Abbey *et al.*, in *UV and X-ray Spectroscopy of Laboratory and Astrophysical Plasmas*, edited by E. Silver and S. Khan (Cambridge University Press, Cambridge, 1993), p. 493.
- ⁹I. M. Melnick Ph.D. thesis, University College, London (1995).
- ¹⁰K. D. Lawson *et al.*, Internal Memo, TAN 96/19, UKAEA Fusion, Culham Laboratory, (1996) (unpublished).
- ¹¹M. A. Singleton, Ph.D. thesis, University College, Cork, Ireland, (1996).
- ¹²R. Willingale, Ph.D. thesis, University of Leicester, (1979).
- ¹³R. Hall, B. Leigh, M. Lewis, and K. D. Evans, *X-ray Spectrometry* **8**, 19 (1979).
- ¹⁴R. A. Hall, Ph.D. thesis, University of Leicester, (1980).
- ¹⁵M. Lewis, P. A. Maksym, and K. D. Evans, *Astron. Astrophys.* **87**, 213 (1980).
- ¹⁶M. Lewis, Ph.D. thesis, University of Leicester, (1982).
- ¹⁷B. L. Henke, E. M. Gullikson, and J. C. Davies, *At. Data Nucl. Data Tables* **54**, 181 (1993).
- ¹⁸N. J. Peacock *et al.*, *Rev. Sci. Instrum.* **66**, 1175 (1995).
- ¹⁹S. Von Goeler *et al.*, *Nucl. Fusion* **15**, 301 (1975).
- ²⁰K. D. Lawson *et al.* (unpublished).
- ²¹J. L. Schwob, A. W. Wooters, S. Suckewer, and M. Finkenthal, *Rev. Sci. Instrum.* **58**, 1601 (1987).
- ²²P. Platz *et al.*, in *Proceedings of the 22nd EPS Conference on Fusion and Plasma Physics, Bournemouth, England*, edited by B. Keen, P. Stott, and J. Winter (JET Undertaking, Abingdon, UK on behalf of European Physical Society, Europhysics Conference Abstracts, 1995), Vol. 19C, part II, p. 385.